Embodied Knowledge Extraction from Human Motion Using Singular Value Decomposition

Yinlai Jiang
School of Systems Engineering,
Kochi University of Technology,
Kami, Kochi 782-8502, Japan.
E-mail: jiang.yinlai@kochi-tech.ac.jp

Isao Hayashi
Faculty of Informatics,
Kansai University,
Takatsuki, Osaka 569-1095, Japan.
E-mail: ihaya@cbii.kutc.kansai-u.ac.jp

Shuoyu Wang
School of Systems Engineering,
Kochi University of Technology,
Kami, Kochi 782-8502, Japan.
E-mail: wang.shuoyu@kochi-tech.ac.jp

***Abstract*—Embodied knowledge is the knowledge remembered by the human body and reflected by the dexterity in the motion of the body. In this paper, we propose a new method using singular value decomposition for extracting embodied knowledge from the time-series data of the motion which is measured with various sensors such as an accelerometer, a motion capture system and a force sensor. We compose a matrix from the the time-series data and use the left singular vectors of the matrix as the patterns of the motion and the singular values as a scalar, by which each corresponding left singular vector affects the matrix. Two experiments were conducted to testify the method. One is a gesture recognition experiment in which we categorize gesture motions by two kinds of models with the indexes of similarity and estimation using left singular vectors. The other is an ambulation evaluation experiment in which we distinguished the levels of walking disability using a 3D hyperplane constructed by the singular values. Finally we discuss the characteristic and significance of the embodied knowledge extraction using singular value decomposition proposed in this paper.**

I. Introduction

Embodied knowledge, sometimes called tacit knowledge, is the skill ability internalized in the body. Embodied knowledge plays an important role in acquiring skills, e.g. for the athletes to moving economically, for the martial artists to make movement more flexible, for the musicians to uplift feeling, and for the ceramists to acquire specific finger sensitivity. Such skill is a native human endowment which is not ordinarily accessible to consciousness.

The information of motion, such as trajectory, speed and acceleration, has been measured to extract and analyze the embodied knowledge [1]–[4]. Time-series data analysis is usually necessary to extract features from the measurement data. Various methods for analysing physical movement have been proposed. Mitra et al. [5] surveyed methods of gesture recognition, and suggested that the Hidden Markov model is effective for gesture motion data analysis. Jerde et al. [6] measured the angles of the hand joints for recognizing fingerspelling hand shapes, and reduced the dimension of hand by discriminant analysis using Principal Component Analysis (PCA). Williamson et al. [7] measured the acceleration of the shank and detected the main phases of normal gait during walking using machine learning. Jakobsen et al. [8] assess knee joint range of motion (ROM) during rehabilitation based on correlation coefficients and smallest real difference. However, the Hidden Markov model is not effective when the number of states is large or the data is discontinuous. Since neural network is too sensitive in time-series data length, the accuracy is not so well. Principal Component Analysis reduces the number of explanatory variables, and is a kind of model for visualization with principal component variables. It is possible however to lose significant principal component variables when the proportion of variance is low and the number of the data is inadequate. The accuracy of PCA declines when the contribution ratio is low due to shortage of data.

In this paper, we propose a new method to extract embodied knowledge of body motion using Singular Value Decomposition (SVD) [9]. The left and right singular vectors, and singular values are decomposed from a Hankel matrix defined from the time-series data. Since the left singular vector represents Hankel matrix characteristics and the singular value means the strength of the left singular vector, it is used more generally as a method for extracting characteristics from observed data. Recently, the SVD has been used in time-series data analysis for data mining [10] and motion analysis to extract similarities and differences in human behavior [11].

We applied the proposed methods to a hand gesture recognition experiment and a walking disability evaluation experiment. In the hand gesture recognition experiment we distinguish 5 kinds of gestures according to the similarity and estimation using the left singular vectors. In the walking disability evaluation experiment we distinguished the levels of walking disability by a three-dimensional hyperplane constructed by the singular values. The characteristic and significance of the embodied knowledge extraction using SVD is discussed based on the results of the two experiments.

II. Embodied Knowledge Extraction Using SVD

Suppose M is an m-by-n matrix, then there exists a factorization of the form:M=$U\Sigma V$, where U=(u_1, u_2, ..., u_m) contains the left singular vectors of M, V=(v_1, v_2, ..., v_n) contains the right singular vectors of M, and the matrix Σ is a m-by-n diagonal matrix with nonnegative real singular values on the diagonal. The SVD is an important factorization of a rectangular real or complex matrix, with many applications in signal processing and statistics. Applications using SVD

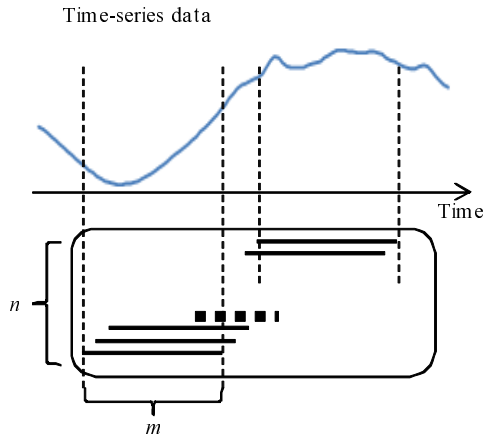

Fig. 1: Design of Matrix $M_X^{i,G}$

include computing the pseudo inverse, least squares data fitting, matrix approximation, and determining the rank, range, and null space of a matrix [9].

Suppose that there are w measurement points $(P_1, P_2, \cdots, P_w)$ on the human body to measure the body motion. On point P_i, the measured data series of the movement G is denoted as $\tau^{i,G}$. The data series of $\tau^{i,G}$ consists of 3-dimentional data $(X^{i,G}, Y^{i,G}, Z^{i,G})$. From this time-series data $\tau^{i,G} = (X^{i,G}, Y^{i,G}, Z^{i,G})$, n vectors by m data sampling are extracted by overlapping, and the matrices $M_X^{i,G}, M_Y^{i,G}$, and $M_Z^{i,G}$ are constructed as a collective of the measurement data on the X, Y, and Z coordinates of the gestures, respectively. Fig. 1 shows the design how to construct the matrix $M_X^{i,G}$. The matrices $M_X^{i,G}, M_Y^{i,G}$, and $M_Z^{i,G}$ are described as follows:

$$M_X^{i,G} = (X_1^{i,G}, X_2^{i,G}, \cdots, X_n^{i,G})^T \quad (1)$$

$$M_Y^{i,G} = (Y_1^{i,G}, Y_2^{i,G}, \cdots, Y_n^{i,G})^T \quad (2)$$

$$M_Z^{i,G} = (Z_1^{i,G}, Z_2^{i,G}, \cdots, Z_n^{i,G})^T \quad (3)$$

where, $X_p^{i,G} = (x_{p,1}^{i,G}, x_{p,2}^{i,G}, \cdots, x_{p,m}^{i,G})$, $p = 1, 2, \cdots, n$, and x is a datum on the X coordinate. We define $Y_p^{i,G}$ and $Z_p^{i,G}$ in the same way.

Suppose $M_k^{i,G}$, $k = \{X, Y, Z\}$ is an m-by-n matrix as general format of $M_X^{i,G}, M_Y^{i,G}, M_Z^{i,G}$. The SVD of the matrix $M_k^{i,G}$ is:

$$M_k^{i,G} = U_k^{i,G} \Sigma_k^{i,G} \{V_k^{i,G}\}^T \quad (4)$$

where $U_k^{i,G} = (u_{1,k}^{i,G}, u_{2,k}^{i,G}, \cdots, u_{m,k}^{i,G})$ is an m-by-m unitary matrix, $\{V_k^{i,G}\}^T$ denotes the conjugate transpose of $V_k^{i,G} = (v_{1,k}^{i,G}, v_{2,k}^{i,G}, \cdots, v_{n,k}^{i,G})$ which is an n-by-n unitary matrix, and the matrix $\Sigma_k^{i,G}$ is a m-by-n diagonal matrix. The diagonal entries of $\Sigma_k^{i,G}$ are the singular values of $M_k^{i,G}$. The matrix $U_k^{i,G}$ contains the left singular vectors of $M_k^{i,G}$ and the matrix $V_k^{i,G}$ contains the right singular vectors of $M_k^{i,G}$.

Now, take $M_X^{i,G}$ as an example of matrix $M_k^{i,G}$ to discuss the motion analysis. The matrix $M_X^{i,G}$ can be decomposed into a product of $U_X^{i,G}$, $\Sigma_X^{i,G}$ and $V_X^{i,G}$ by the SVD. Intuitively, the left singular vectors in $U_X^{i,G}$ form a set of patterns of $M_X^{i,G}$ and the diagonal values in matrix $\Sigma_X^{i,G}$ are the singular values, which can be considered as scalars by which each corresponding left singular vectors affect the matrix $M_X^{i,G}$. Suppose that the number of left singular vectors is l, and the element number of the j th left singular vector is q. Let us denote the couples of the singular values and the left singular vector as $((\sigma_{1,X}^{i,G}, u_{1,X}^{i,G}), (\sigma_{2,X}^{i,G}, u_{2,X}^{i,G}), \cdots, (\sigma_{l,X}^{i,G}, u_{l,X}^{i,G}))$, for $u_{j,X}^{i,G} = (\hat{u}_{1j,X}^{i,G}, \hat{u}_{2j,X}^{i,G}, \cdots, \hat{u}_{hj,X}^{i,G}, \cdots, \hat{u}_{qj,X}^{i,G})$ in the descending order of the singular values, where $\hat{u}_{hj,X}^{i,G}$ is the h th element of the j th left singular vector$u_{j,X}^{i,G}$. The left singular vector expresses the characteristic of the whole time-series data better if its corresponding singular value singular is larger. That is, the greater the singular value is, the more dominant the corresponding pattern is.

III. Gesture Recognition with Left Singular Vectors

The left singular vectors $(u_{1,X}^{i,G}, u_{2,X}^{i,G}, \cdots, u_{l,X}^{i,G})$ represent the characteristic of hand gestures well. We conducted a gesture recognition experiment to demonstrate the effectiveness of feature extraction using the left singular vectors.

A. Hand Gesture Measurement Using Left Singular Vectors

5 kinds of hand gestures, CH (Come here), GA (Go away), GR (Go right), GL (Go left), and CD (Calm down), were performed by two subjects, SW and ST, who were male in their 20s. These gestures are commonly used in daily life for guidance. The gestures were performed in a $50cm \times 50cm \times 50cm$ cubic space, whose zero point and coordinate system are shown in Fig. 2. The motions of the hand gestures are measured with Movetr/3D and GE60/W (Library, Tokyo, Japan). Five markers, M_1 on the tip of the thumb, M_2 on the tip of the middle finger, M_3 on the tip of the little finger, M_4 on the thumb-side of the wrist and M_5 on the little finger side of the wrist, were measured.

The motion of subject SW performing CH is shown in Figure 3 by 9 frames extracted from the experiment video every 1/6 s. The measurement time-series data of M_2 when subject SW performed the five kinds of gestures are shown in Figure 4. In Figure 4, a movement change as for GA, CH, and CD is big in the top and bottom direction (onto z-axis) and in the front and back direction (onto y-axis), and as for GR and GL, the movement change is big in the right and left direction (onto x-axis).

One gesture was executed 9 times by each subject. Data of the first 5 times execution were used as acquisition of patterns of the gesture. Data of last 4 times were used to be distinguished.

We proposed two kinds of gesture recognition methods using the left singular vectors extracted from the time-series data of gesture motion: gesture recognition based on the similarity between gesture distances and gesture recognition based on the similarity between gesture vectors .

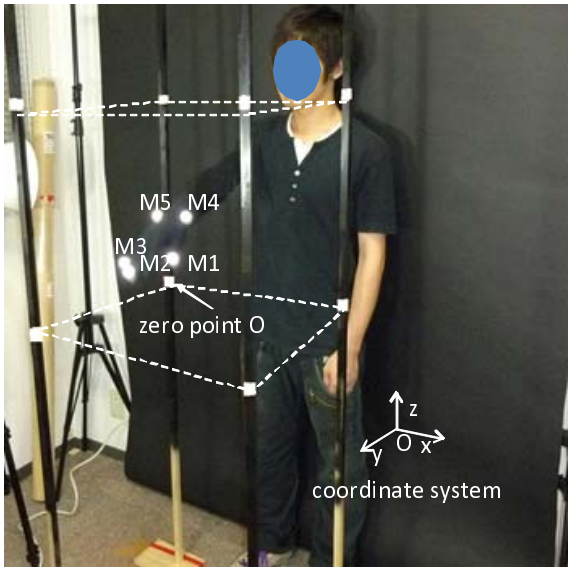

Fig. 2: Experiment Environment

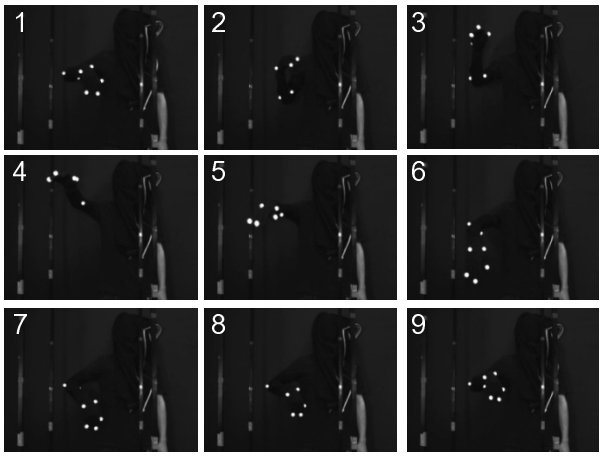

Fig. 3: Example of Gestures

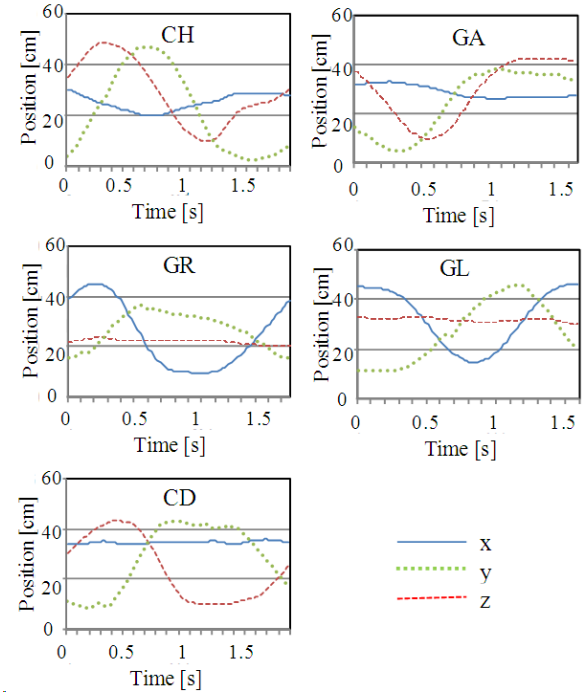

Fig. 4: Five Kinds of Hand Gestures

B. Gesture Recognition based on Similarity between Gesture Distances

Suppose that the observed data series are divided into two groups: $\tau^{i,G}_{TRD}$ as training data series, and $\tau^{i,G}_{CHD}$ as checking data series. Let us denote the left singular vector $\tau^{i,G}_{X,TRD}$ for training data related to the X coordinate values of the point P_i on the hand for the gesture G as $U^{i,G}_{X,TRD} = (u^{i,G}_{1,X,TRD}, u^{i,G}_{2,X,TRD}, \cdots, u^{i,G}_{l,X,TRD})$ for $u^{i,G}_{j,X,TRD} = (\hat{u}^{i,G}_{1j,X,TRD}, \hat{u}^{i,G}_{2j,X,TRD}, \cdots, \hat{u}^{i,G}_{hj,X,TRD}, \cdots, \hat{u}^{i,G}_{qj,X,TRD})$. We define the left singular vectors $\tau^{i}_{X,CHD}$ for checking data as $U^{i}_{X,CHD} = (u^{i}_{1,X,CHD}, u^{i}_{2,X,CHD}, \cdots, u^{i}_{l,X,CHD})$, for $u^{i}_{j,X,CHD} = (\hat{u}^{i}_{1j,X,CHD}, \hat{u}^{i}_{2j,X,CHD}, \cdots, \hat{u}^{i}_{hj,X,CHD}, \cdots, \hat{u}^{i}_{qj,X,CHD})$ in the same way.

To recognize hand gesture, three kinds of similarity criteria are defined on the data $\tau^{i,G} = (X^{i,G}, Y^{i,G}, Z^{i,G})$ as follows;

$$S_1 : r_i(U^{i,G}_{TRD}, U^{i}_{CHD}) = \frac{1}{3lq}\sum_{k=1}^{3}\sum_{j=1}^{l}\left|\sum_{h=1}^{q}\hat{u}^{i,G}_{hj,k,TRD} - \sum_{h=1}^{q}\hat{u}^{i}_{hj,k,CHD}\right| \quad (5)$$

$$S_2 : r_i(U^{i,G}_{TRD}, U^{i}_{CHD}) = \frac{1}{3lq}\sum_{k=1}^{3}\sum_{j=1}^{l}\sum_{h=1}^{q}|\hat{u}^{i,G}_{hj,k,TRD} - \hat{u}^{i}_{hj,k,CHD}| \quad (6)$$

$$S_3 : r_i(U^{i,G}_{TRD}, U^{i}_{CHD}) = \frac{1}{3lq}\sum_{k=1}^{3}\sqrt{\sum_{j=1}^{l}\sum_{h=1}^{q}(\hat{u}^{i,G}_{hj,k,TRD} - \hat{u}^{i}_{hj,k,CHD})^2} \quad (7)$$

The similarity S_1 is defined by the absolute differential of the total left singular vector between the training data and the checking data. The similarity S_2 is defined by the total absolute differential of the left singular vectors between the training data and the checking data at the same order. The similarity S_3 is defined by the Euclidean distance between the left singular vectors of the training data and the checking data on the multidimensional space.

Since there are w measurement points $(P_1, P_2, \cdots, P_w)$, the estimated gesture G^* is identified by the following two kinds

TABLE I: Recognition of Gestures

	Similarity (S_1)	Similarity (S_2)	Similarity (S_3)
Estimation (E_1)	70.0	90.0	80.0
Estimation (E_2)	60.0	80.0	80.0

of estimations;

$$E_1 : G^* = \{G_f | \max_f \sum_{i=1}^{w} n(G_f^i), \quad for \;\; G_f^i = \{G_f | \min_f r_i(U_{TRD}^{i,G_f}, U_{CHD}^i)\}\} \tag{8}$$

$$E_2 : G^* = \{G_f | \min_f \sum_{i=1}^{w} r_i(U_{TRD}^{i,G_f}, U_{CHD}^i)\} \tag{9}$$

where, G_f is the f th gesture among the five hand gestures, and $n(G_f^i)$ is a counting function which is $n(G_f^i) = 1$ if the condition G_f^i is satisfied at the P_i point on the hand.

The estimation E_1 is defined for gesture by counting the large number of minimal similarity values. The estimation E_2 is defined by the minimal total similarity values.

Table I shows the recognition results among both of the two subjects' gesture patterns based on the three kinds of difference similarities, Equation (5), Equation (6) and Equation (7). In the calculation, $m = 125, n = 5, q = 125, l = 1, w = 5$. The recognition results suggest that the similarity S_2 and S_3 leaded to relatively higher correct recognition rates. Especially, the pair of the similarity S_2 and the estimation E_1 leads to a significantly high accuracy of 90.0%. The result suggests that the pair of S_2 and E_1 is more feasible to be used in gesture recognition. However, in general it is hard to distinguish between a gesture of GR (Go Right) and GL (Go Left), and so the results are understandable.

In the experiment, the positions of the five markers on the right hand were measured. However, it is possible that not all the positions of these markers may have a high relevance to the gestures. Reducing the number of markers considered in the recognition might not only reduce the calculation but also improve the recognition accuracy. Next, by calculating the left singular vectors at each markers, we compared the accuracy on each marker for gesture recognition with similarity S_2 and estimaiton E_1. Table II shows the large counting number of minimized similarity values. As a result, the first marker M_1 was selected as the most important marker because the accuracy is 93.85%, and the highest. Since M_1 measures the time series at the tip of the thumb and it's largely related to movement of the thumb, it is suggested that the motion of the thumb is important in gesture recognition.

C. Method for Similarity between Gesture Vectors

As for the second method, gesture recognition is based on the similarity between gesture vectors. Now, consider the data

TABLE II: Comparison of Markers by Gesture Distances

Sub./Ges.	Markers				
TW	M_1	M_2	M_3	M_4	M_5
CH	4/GA	4/GA	4/CD	4/GA	4/GA
GA	8/GA	9/GA	9/GA	8/GA	8/GA
GR	7/GR	8/GR	8/GR	6/GR	5/GR*
GL	5/GL	4/GL*	4/GL*	5/GL	5/GL
CD	6/CD	5/GA	5/GA	7/CD	8/CD
ST	M_1	M_2	M_3	M_4	M_5
CH	8/CH	9/CH	11/CH	9/CH	7/CH
GA	7/GA	9/GA	9/GA	9/GA	5/CD
GR	9/GR	10/GR	11/GR	6/GR	9/GR
GL	7/GL	8/GL	10/GL	5/GL	8/GL
CD	4/CD*	5/GL	5/GL	5/CD	6/CD
Accuracy (%)	93.85	80.28	81.58	93.75	86.15

series in $M_X^{i,G}$ of Equation (1). If one of the data series $X_p^{i,G}$ is replaced by another data series X_{CHD}^i, the singular values and left singular vectors of $M_{X,CHD}^i$, will be different from those of $M_X^{i,G}$.

$$M_{X,CHD}^i = (X_1^{i,G}, \cdots, X_{p-1}^{i,G}, X_{CHD}^i, X_{p+1}^{i,G}, \cdots, X_n^{i,G})^T \tag{10}$$

The difference between the left singular vectors of $M_X^{i,G}$ and $M_{X,CHD}^i$ is determined by how X_{CHD}^i is different from the other $p-1$ data series. The patterns of $M_{X,CHD}^i$ will change more when $X_p^{i,G}$ is replaced by a quite dissimilar data series than when it is replaced by a similar one. Therefore, the difference between the left singular vectors of $M_X^{i,G}$ and X_{CHD}^i can be considered as a measure of the difference between X_{CHD}^i and the other data series. If X_{CHD}^i comes from another kind of hand gesture, the difference can be utilized as a criterion for judging whether X_{CHD}^i comes from the same kind of hand gesture as the other data series. In our algorithm, the location of X_{CHD}^i is fixed in the end of data series. Therefore, only the n th $X_n^{i,G}$ is replaced by another data series X_{CHD}^i in Equation (10).

To recognize hand gesture, three kinds of similarity criteria are defined on the data $\tau^{i,G} = (X^{i,G}, Y^{i,G}, Z^{i,G})$ as follows:

$$S_4 : r_i(U_{TRD}^{i,G}, U_{CHD}^i) = \frac{1}{3lq} \sum_{k=1}^{3} \sum_{j=1}^{l} |\sum_{h=1}^{q} \hat{u}_{hj,k,TRD}^{i,G} - \sum_{h=1}^{q} \hat{u}_{hj,k,CHD}^{i}| \tag{11}$$

$$S_5 : r_i(U_{TRD}^{i,G}, U_{CHD}^i) = \frac{1}{3lq} \sum_{k=1}^{3} \sum_{j=1}^{l} \sum_{h=1}^{q} |\hat{u}_{hj,k,TRD}^{i,G} - \hat{u}_{hj,k,CHD}^{i}| \tag{12}$$

$$S_6 : r_i(U_{TRD}^{i,G}, U_{CHD}^i) = \frac{1}{3lq} \sum_{k=1}^{3} \sqrt{\sum_{j=1}^{l} \sum_{h=1}^{q} (\hat{u}_{hj,k,TRD}^{i,G} - \hat{u}_{hj,k,CHD}^{i})^2} \tag{13}$$

TABLE III: Results of Method for Similarity between Gesture Vectors

Sub.	Ges.	Similarity (S_4)	Similarity (S_5)	Similarity (S_6)
TW	CH	1	2	1
	GA	3	4	4
	GR	2	3	3
	GL	1	3	3
	CD	0	3	3
ST	CH	2	2	2
	GA	1	4	4
	GR	3	4	4
	GL	0	3	2
	CD	0	4	4
Accuracy (%)		30.3	80.0	75.0

TABLE IV: Comparison of Markers by Gesture Vectors

Sub./Ges.	Markers				
TW	M_1	M_2	M_3	M_4	M_5
CH	2/GA	2/GA	2/GA	3/GA	2/GA
GA	4/GA	4/GA	2/GA*	4/GA	4/GA
GR	3/GR	3/GR	3/GR	3/GR	3/GR*
GL	3/GL	3/GL	3/GL	3/GL	3/GL
CD	3/CD	2/GA	3/GA	2/CD	2/CD
ST	M_1	M_2	M_3	M_4	M_5
CH	2/CH*	2/CH*	2/CH*	2/CH*	2/CH*
GA	4/GA	4/GA	4/GA	4/GA	4/CD
GR	4/GR	4/GR	4/GR	3/GR	3/GL
GL	4/GL	4/GL	4/GL	3/GR	4/GR
CD	4/CD	4/CD	4/CD	3/CD	4/CD
Accuracy (%)	93.94	87.50	83.87	80.00	58.06

The meanings of S_4, S_5, and S_6 are the same as those of S_4, S_5, and S_6 respectively. Since there are w measurement points $(P_1, P_2, \cdots, P_w)$, the estimated gesture G^* is identified by the following estimations:

$$E_3 : G^* = \{G_f | \min_f \sum_{i=1}^{w} r_i(U_{TRD}^{i,G_f}, U_{CHD}^{i})\} \qquad (14)$$

In the proposed method, all of the time series must have the same number of data in order to compose matrix $M_X^{i,G}$ as shown in Equation (1). However, the lengths of the hand gestures in real measurement are different according the kinds of gestures and the subjects to perform them. Therefore, preprocessing is necessary to make the data series have the same number of data. In this paper, the number of data was set to be the average number. If a data series contains more data than the average number, data are deleted from the data series at the same interval. If a data series contains fewer data than the average number, data are interpolated in to the data series at the same interval. The interpolated data are calculated using quadric interpolation.

Table III shows the recognition results based on the three kinds of similarity definitions of S_4, S_5, and S_6, in Equation (11), Equation (12), and Equation (13) respectively. The recognition results suggest that similarity definitions of S_5 and S_6 leaded to relatively higher correct recognition rates while the correct rate of the recognition based on S_4 was very low. Therefore, S_5 and S_6 are more feasible in gesture recognition.

As same as comparison of makers in the method by similarity between gesture distances, we compared the accuracy of markers in this method by similarity between gesture vectors with similarity S_5 and estimaiton E_3. Table IV shows the large counting number of minimized similarity values. The first M_1 was selected as the most important marker as same as Table II. We realize that the movement of thumb is greatly related to gesture recognition by the results.

D. Discussions

The recognition results of the two method show that the left singular vectors extracted from the time-series data can be used as knowledge to distinguish gestures. Especially, the total absolute differential of a left singular vectors at the same order is significantly effective because the left singular vectors expresses a time-dependent weight for identifying the whole movement. Regarding the incorrect recognitions, motion data was quite similar although the motion was incorrectly recognized as a gesture different from the intended one. Gestures GR and GL, for example, have the opposite meanings but their motions are very similar in that the hand waves left and right. Their difference lies in that the hand moves faster from left in to right in GR while faster from right to left in GL. Even human beings sometimes mistake distinguishing between them.

IV. Walking Disability Evaluation Using Singular Values

A. Acceleration Measurement with Wearable Wireless Accelerometers

The acceleration is measured by 3 wearable wireless 3-axis accelerometers (Motion Recorder MVP-RF8, Microstone Nagano, Japan): M1 on the back of the waist (B. Waist), M2 on the midpoint of the right shank (R. M. Shank), and M3 on the midpoint of the left shank (L. M. Shank), as shown in Fig. 5. Sampling rate of the sensor was 100 Hz. When the subject stands upright, the sensors' x-axis is front/back, y-axis up/down, and z-axis right/left. However, since the orientation of the sensors changes during walking, the coordination system will also change. In the experiment, we examined the acceleration of walking difficulty simulated by restricting the right leg with knee supporters and weight bands (Fig. 5). The knee supporter bound around the knee joint decrease the range of movement (ROM) of the knee joint and

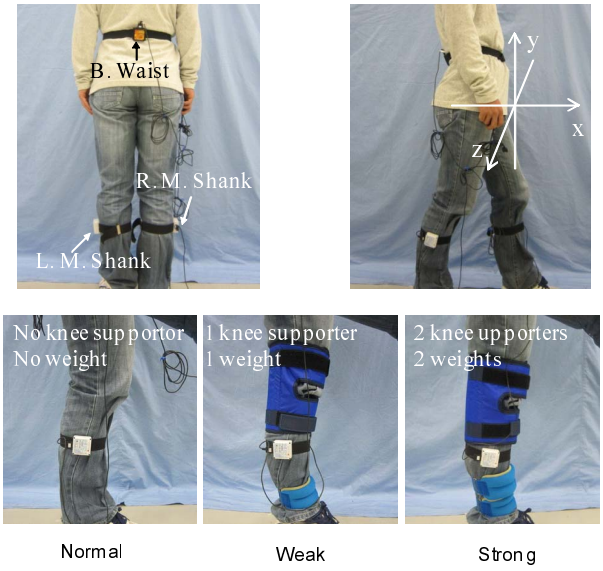

Fig. 5: Experiment settings for ambulation

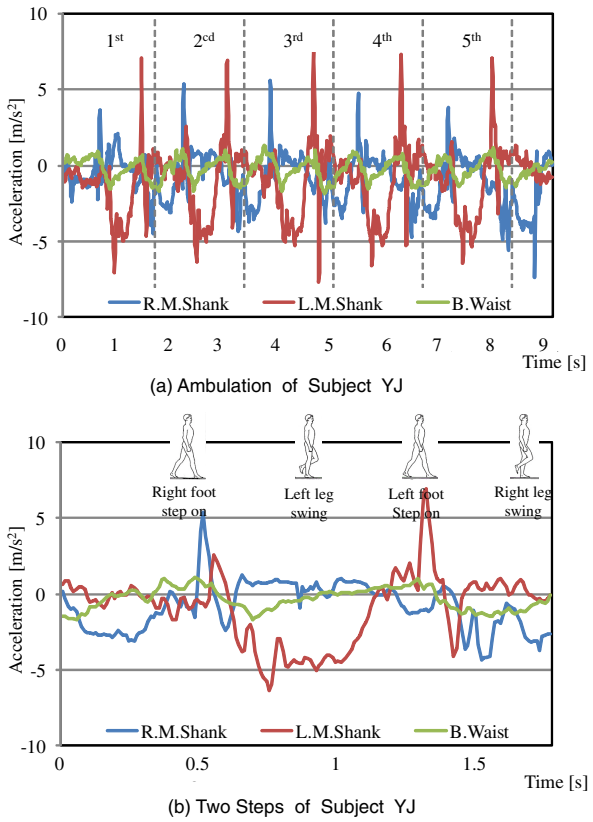

Fig. 6: Example of Ambulation

the weight band bound around the ankle joint can simulate the weakness in muscle strength. The simulation is very important in testing our method since it does not endanger the safety of the disabled during the development phase of the method. Two levels of walking difficulty were simulated by two levels of restraint in the experiment. Weak restraint was simulated with one knee supporter and one weight band (1 kg), and strong restraint with two knee supporters and two weight bands (2 kg). Totally, 3 statuses (Normal without restraint, Weak, and Strong) were examined.

Six healthy volunteers (YJ, TK, KT, KS, TF, and RT, 5 males and 1 female) aged 21-31 yr (mean 26 yr) participated in the experiment. Subjects were instructed to walk straight about 4m along a straight line. The experiment was carried in the status order of Normal, Weak, and Strong. For each status, each subject walked 4 times.

The measurement time-series data in x coordinate of the three sensors when subject YJ walked in the status of Weak are shown in Fig. 6. The fluctuation of the acceleration was significant when the right foot or the left foot landing. There are 5 strides in Fig. 6a. Acceleration data of the first stride are extracted and shown in Fig. 6b. All the acceleration at the B. Waist, R. M. Shank, and L. M. Shank significantly fluctuated when the right foot pushed off from the floor or stepped on the floor. The fluctuation in the acceleration at L. M. Shank was more significant than that at R. M. Shank since the right leg was restricted by the knee supporter and the weight band. The fluctuation in the acceleration at B. Waist was the smallest among the three measurement points. This showed that the trunk of the body, especially the waist, was relatively kept stable to maintain the body balance even when there is disability in lower limbs.

B. Relationship between Singular Values and Walking Disability

We focused on the acceleration change around the time when the right foot pushed off and stepped on the floor. The acceleration data around right foot landing were analyzed. The matrix M for the SVD was designed according to the local maximum turning points, as shown in Fig. 6. It took 5 strides to walk 4 m in the experiment. Acceleration data of the middle 3 strides, which do not involve the initiation and termination of the walking movement, were extracted for analysis. The data from 0.5s before the maximum turning point to 0.5s after the maximum turning point were extracted as column vectors. For each turning point, 9 column vectors (3 sensors, each has 3 coordinates) were extracted. The column vectors from the same acceleration data series composed a matrix M. Therefore, M was a matrix of 100 rows and 3 columns. In this paper, only the first singular value and the first left singular vector were considered. Thus parameter l was 1.

The first singular values extracted from the acceleration data with SVD are listed in Table V. In spite of the individual differences in walking, similar singular value changes of all the 6 subjects were shown. The singular values of M2 and M3 decreased with the increase of walking difficulty, especially those of M2 decreased in all the X, Y and Z axes. However, the decrease did not show at M1. Waist is the center of the body and is always kept balanced during movement. Fig. 6 shows that the waist was relatively kept stable to maintain the

TABLE V: Singular Value of Ambulation Experiment

Subjects	Restraint Ambulation	M_1			M_2			M_3		
		X	Y	Z	X	Y	Z	X	Y	Z
TF	Normal	17.7	23.4	21.8	57.9	52.7	50.9	46.8	55.6	33.4
	Weak	17.0	23.3	26.9	33.3	34.7	39.4	42.5	48.0	28.4
	Strong	17.6	22.8	27.3	31.7	30.3	37.7	40.4	43.1	27.8
YJ	Normal	11.4	9.4	12.1	45.9	40.5	22.2	47.3	48.2	18.9
	Weak	10.9	8.2	15.4	23.4	11.2	13.9	43.9	33.5	14.7
	Strong	18.3	10.4	18.5	19.5	10.2	13.0	42.0	25.6	13.7
TK	Normal	18.1	19.3	12.6	51.1	34.3	34.0	51.9	47.8	30.1
	Weak	20.6	20.4	17.0	27.5	25.1	26.4	45.7	45.8	27.3
	Strong	20.2	20.0	15.7	25.3	20.1	21.9	42.8	38.5	27.7
KS	Normal	20.2	19.0	12.8	60.4	58.8	36.3	57.3	66.4	25.8
	Weak	19.7	15.8	19.0	36.8	32.0	21.5	52.4	55.0	20.1
	Strong	18.8	15.9	19.2	33.5	29.3	18.9	39.6	34.6	19.3
RT	Normal	28.0	24.5	19.6	70.8	53.7	37.5	58.7	58.0	32.5
	Weak	24.5	22.3	17.8	60.7	34.9	27.3	56.9	58.1	30.4
	Strong	22.5	23.7	19.1	51.5	33.3	20.8	50.3	52.7	26.1
KT	Normal	23.4	27.5	17.9	57.1	65.3	40.3	60.6	74.3	32.0
	Weak	21.6	31.5	24.3	40.3	37.4	25.4	46.0	59.6	22.1
	Strong	18.5	24.3	22.4	38.5	26.8	16.0	38.5	46.4	16.4
Ave.	Normal	19.8	20.5	16.1	57.2	50.9	36.9	53.8	58.4	28.8
	Weak	19.1	20.3	20.1	37.0	29.2	25.7	47.9	50.0	23.8
	Strong	19.3	19.5	20.4	33.3	25.0	21.4	42.3	40.2	21.8

body balance. The first singular values of M2, therefore, are suggested to be effective criteria to evaluate walking difficulty. That is, the first singular values from the acceleration of the restricted leg decreases with the increase of walking difficulty.

C. R-Plane for Visualization of Walking Disability

The results in Table V show the possibility of evaluating walking disability using the singular values. In order to provide a more understandable presentation of the data for the physical therapists and the patients, we propose a visualization tool, a rehabilitation plane (R-Plane), to assist in the evaluation of walking disability.

The first singular values extracted from the acceleration data at M2 are plotted in a 3D space in Fig. 7. The singular values of the 4 times of walking are plotted in different shape and color according to the 3 statuses. The average singular values of the 3 statuses are connected by black lines. Fig. 7 shows that the first singular values are clustered according to the statuses. The line connecting the average values can be considered as severity line of walking difficulty. A plane can be defined by the average singular values of the 3 statuses. Given a patient's singular values of walking, draw a perpendicular line from the point defined by the singular values to the lines connecting the average singular values, then the patient's walking disability can be evaluated intuitively by the position of the intersection

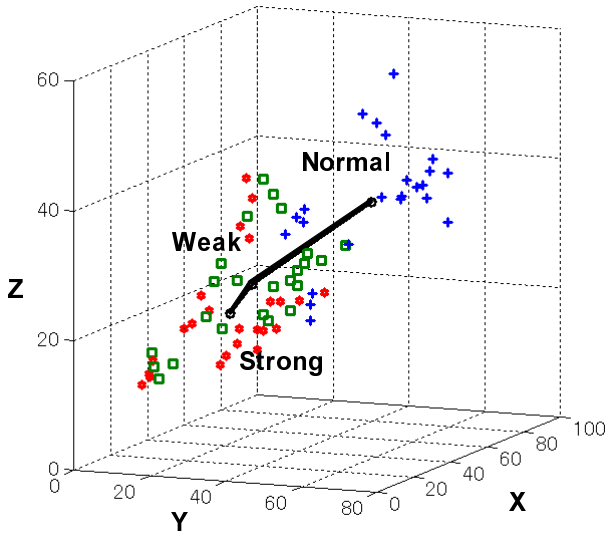

Fig. 7: Singular Values of the 3 Statuses

point. The plane is called a R-Plane which can be used for walking disability evaluation in rehabilitation to assess the recovery of the patients.

The conceptual diagram of the R-Plane is shown in Fig. 8.

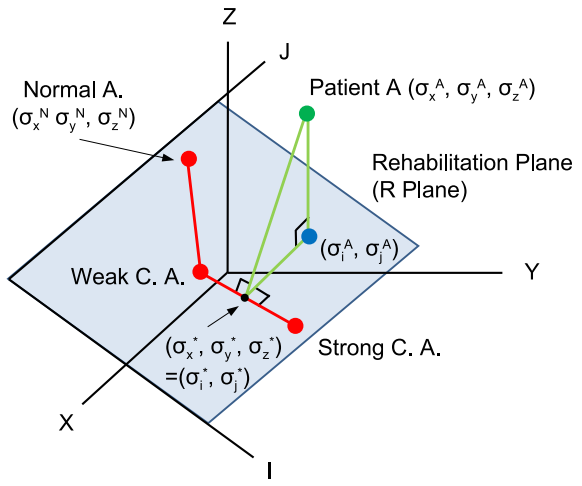

Fig. 8: Conceptual diagram of R-Plane

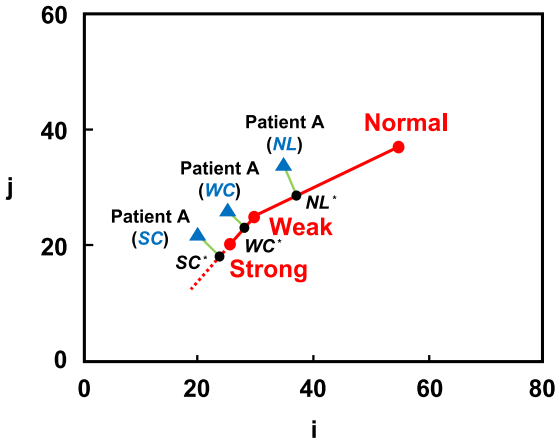

Fig. 9: Example of R-Plane

Suppose the normal vector of the R-Plane is $\vec{n} = (n_x, n_y, n_z)$ and the average singular values of the status Normal is $(\sigma_x^N, \sigma_y^N, \sigma_z^N)$, the R-Plane can be described by Equation (15).

$$n_x(x - \sigma_x^N) + n_y(y - \sigma_y^N) + n_z(z - \sigma_z^N) = 0 \qquad (15)$$

Suppose the coordinates of patient A in the 3D space are $(\sigma_X, \sigma_Y, \sigma_Z)$ whose projection to the R-Plane is (σ_i^R, σ_j^R). The projection of (σ_i^R, σ_j^R) to the line connecting the average singular values is $(\sigma_i^*, \sigma_j^*) = (\sigma_X^*, \sigma_Y^*, \sigma_Z^*)$. Then the walking disability and recovery of patient A can be assessed by the position of (σ_i^*, σ_j^*) and the distances of (σ_i^R, σ_j^R) to the average singular values.

As an example, take subject TK as the patient A and draw the R-Plane based on the average singular values of the other 5 subjects. The equation of the plane is

$$-0.810x + 0.532y + 0.246z + 9.284 = 0 \qquad (16)$$

The R-Plane is shown in Fig. 9. Subject TK's singular values in the statuses of Normal, Weak, Strong are (NL, WC, SC) whose projection to the lines in the R-Plane are (NL^*, WC^*, SC^*). Although status Normal is not so accurately, Statuses Weak and Strong are correctly located in the figure. The results show the effectiveness of the R-Plane in intuitively presenting the walking disability and providing visual information of the patient's recovery.

V. Conclusion

A new method for embodied knowledge extraction from the time-series data of motion is proposed based on the SVD. The effectiveness of the method was shown by the gesture recognition using the left singular vectors and the walking disability evaluation using the singular values.

Acknowledgment

This work was supported by Strategic Project to Support the Formation of Research Bases at Private Universities: Matching Fund Subsidy from MEXT (Ministry of Education, Culture, Sports, Science and Technology), 2008-2012, and Grants-in-Aid for Scientific Research Nos. 20240058 and 21300212 from the Japan Society for the Promotion of Science.

References

[1] R. Balasubramaniam and M. T. Turvey, "Coordination Modes in the Multisegmental Dynamics of Hula Hooping," *Biological Cybernetics*, vol.90, pp. 176-190, 2004.

[2] Hirashima M, Kudo K, Watarai K and Ohtsuki T, "Control of 3D limb dynamics in unconstrained overarm throws of different speeds performed by skilled baseball players," *Journal of Neurophysiology*, vol.97, pp.680-691, 2007.

[3] Nakayama Y, Kudo K and Ohtsuki T, "Variability and fluctuation in running gait cycle of trained runners and non-runners. *Gait & Posture*, 31: 331-335, 2010.

[4] S. Furuya, R. Osu, and H. Kinoshita, "Effective Utilization of Gravity During Arm Downswing in Keystroke by Expert pianists," *Neuroscience*, vol.164, no.2, pp. 822-831, 2009.

[5] S.Mitra, and T.Acharya, "Gesture recognition: a survey," *IEEE Transactions on Systems, Man, and Cybernetics, Part C*, vol.37, no.3, pp.311-324, 2007.

[6] T.E.Jerde, J.F.Soechting, and M.Flanders, "Biological Constraints Simplify the Recognition of Hand Shapes," *IEEE Transactions on Biomedical Engineering*, vol.50, no.2, pp.265-269, 2003.

[7] R.Williamson, and B.J.Andrews, "Gait Event Detection for FES Using Accelerometers and Supervised Machine Learning," *IEEE Transactions on Rehabilitation Engineering*, vol.8, no.3, pp.312-319, 2000.

[8] T.L.Jakobsen, M.Christensen, S.S.Christensen, M.Olsen, and T.Bandholm, "Reliability of Knee Joint Range of Motion and Circumference Measurements after Total Knee Arthroplasty: Does Tester Experience Matter?," *Physiotherapy Research International*, vol.15, no.3, pp.126-134, 2010.

[9] M.E.Wall, A.Rechtsteiner, and L.M.Rocha, "Singular Value Decomposition and Principal Component Analysis." in *A Practical Approach to Microarray Data Analysis*, D.P. Berrar, W. Dubitzky, and M.Granzow, eds. pp.91-109, Kluwer, 2003.

[10] T.Ide, and K.Inoue, "Knowledge Discovery from Heterogeneous Dynamic Systems Using Change-point Correlations," *Proc. 2005 SIAM International Conference on Data Mining (SDM05)*, pp.571-576, 2005.

[11] K. Mishima, S. Kanata, H. Nakanishi, T. Sawaragi and Y. Horiguchi, "Extraction of similarities and differences in human behavior using singular value decomposition," *Proc. of The 11th IFAC/IFIP/IFORS/IEA Symposium on Analysis, Design, and Evaluation of Human-Machine Systems*, 2010.